

The galactic abundance gradient from Cepheids

IV. New results for the outer disc^{*,**}

R. E. Luck¹, W. P. Gieren², S. M. Andrievsky^{3,4}, V. V. Kovtyukh^{3,4}, P. Fouqué⁵, F. Pont⁶, and F. Kienzle⁶

¹ Department of Astronomy, Case Western Reserve University, 10900 Euclid Avenue, Cleveland, OH 44106-7215, USA
e-mail: luck@fafnir.astr.cwru.edu

² Departamento de Física, Grupo de Astronomía, Universidad de Concepción, Casilla 160-C, Concepción, Chile
e-mail: wgieren@coma.cfm.udec.cl

³ Department of Astronomy, Odessa State University, Shevchenko Park, 65014 Odessa, Ukraine
e-mail: val@deneb.odessa.ua

⁴ Odessa Astronomical Observatory and Isaac Newton Institute of Chile, Odessa Branch, Ukraine

⁵ European Southern Observatory, Casilla 19001, 19 Santiago, Chile
e-mail: pfouque@eso.org

⁶ Geneva Observatory, 1290 Sauverny, Switzerland
e-mail: Frederic.Pont@obs.unige.ch; Francesco.Kienzle@obs.unige.ch

Received 8 October 2002 / Accepted 22 January 2003

Abstract. As a continuation of our previous work on the abundance gradient in the outer part of the galactic disc, this paper presents results on the metallicity distribution over galactocentric distances up to 15 kpc. The outer disc is clearly separated from the middle part by the existence of a step in the metallicity distribution at about 10 kpc. Taking the region of galactocentric distances from 10 kpc to 15 kpc, one can derive an iron gradient -0.03 ± 0.01 dex kpc⁻¹ (25 stars). The existence of a discontinuity can be caused by the effective suppression of mixing processes near the corotation circle where the radial component of the gas velocity should be very small.

Key words. stars: abundances – stars: variables: Cepheids – Galaxy: abundances – Galaxy: evolution

1. Introduction

Van den Bergh (1958) was perhaps the first to provide a strong theoretical argument that a metallicity gradient should exist in the galactic disc. During the following almost fifty years many observational studies have been performed with the intent of determining the gradient. Astronomers have analyzed the spectra of B stars, late-type supergiants, old disk giants, and PNe and H II regions, frequently producing rather contradictory results. According to some studies, a quite steep present-day metallicity gradient exists in the disc (from -0.05 to -0.10 dex kpc⁻¹), but much lower gradient values have also been reported, and even no dependence of the abundances upon the galactocentric distances was found in several surveys (see

the brief description of the gradient history in Andrievsky et al. 2002a).

Working in parallel with the observers, theoreticians have made numerous attempts to elaborate a working model of galactic chemodynamics in order to reproduce the observed gradients. Although the different models are based on quite different input physics and assumptions, the actual differences in their predictions concerning the behavior of the present radial elemental distributions appears to be much smaller than the range of observational uncertainties (see e.g. Chiappini et al. 2001). Based on the available observations, a critical choice between the models has thus far been impossible.

In a series of papers, Andrievsky et al. (2002a–c) – hereafter Papers I–III, have reported on the results of a high-accuracy study of the galactocentric metallicity gradient based on the use of Cepheid variables. Cepheids are stars with well-defined distances that can provide radial elemental distributions for chemical elements from carbon to gadolinium.

Cepheids are rather young galactic objects having masses ranging from approximately $12 M_{\odot}$ to $4 M_{\odot}$ which corresponds

Send offprint requests to: S. M. Andrievsky,
e-mail: scan@deneb.odessa.ua

* Based on spectra collected at the New Technology Telescope at ESO - La Silla, Chile, under programme 68.D-0201(B).

** Table A.1 is only available in electronic form at
<http://www.edpsciences.org>

to ages of about 2×10^7 – 3×10^8 yr (very roughly the age of Cepheid can be estimated as the life-time of its main-sequence progenitor, i.e. $t \sim 10^{10} (M/M_{\odot})^{-2.5}$ yr, Lang 1974). Therefore, these stars trace the present-day abundance gradient in the ISM. Of the elements whose abundance can be measured from Cepheid spectra only C, N, Na (and perhaps Mg and Al) are expected to have abundances modified through previous evolution due to the operation of CNO-, NeNa-, MgAl- cycles and dredge-up. The remainder of the elements in Cepheids should have abundances that reflect the ISM from which these stars were recently formed.

According to our results, the elemental distributions display a complicated structure indicating that a single gradient value may be insufficient to represent the observational data over the large observed range of galactocentric distances. One of the prominent features of the radial distributions is the abrupt discontinuity in metallicity seen at $R_G = 10$ kpc. All seventeen stars with galactocentric distances from 10 kpc to 12 kpc investigated in Paper III are metal deficient with a mean $[\text{Fe}/\text{H}] \approx -0.2$. With the aim of extending our previous study of the metallicity distribution in the outer disc towards even larger galactocentric distances, and to better sample this region, we have carried out additional observations of a number of more distant Cepheids. These new observations of metal-poor outer disc Cepheids will also be very useful in a test of the metallicity dependence of Cepheid absolute magnitudes with the infrared surface brightness technique (Gieren et al. 1997, 1998; Pont et al. 2001).

2. Observations and data reduction

The observations were carried out on 11 and 12 January 2002 with the 3.5-m NTT telescope at La Silla (ESO, Chile). The EMMI echelle spectrograph in its red arm configuration with grating # 10 and grism # 3, equipped with a 2048×2048 CCD was used. The resolving power in this setup was about 28 000. The maximum exposure time for one spectrum was 45 min. The spectra have S/N ratios in the range from about 40 to 100, with the fainter stars having the lower signal to noise ratios. Table 1 contains details concerning our program Cepheid observations as well as some information about the Cepheids themselves.

The spectra were extracted from the raw frames using standard IRAF procedures including scattered light subtraction. The original data frames were subframed to extract only the spectral region from 4500 to 8000 Å. Order ends were also clipped to retain only the central regions. Even with this latter clipping there is significant overlap from order to order in wavelength. After extraction the spectra were continuum normalized, wavelength calibrated, and had equivalent widths measured using the ASP package developed by R. E. Luck. Comparison of equivalent widths determined from adjacent orders indicates that the measures are accurate at the 5% level above 100 mÅ. As an example, in Fig. 1 we show two fragments of the spectra for two Cepheids with different metallicities.

3. Atmospheric parameters, abundances, and distances

In Paper I the pertinent details concerning the determination of atmospheric parameters and elemental abundances can be found along with a description of our method of estimating the galactocentric distances. The same methods were used in Papers II and III. The analysis code used was LINES (Snedden 1973) which has been extensively modified/expanded by R.E. Luck. This code has been benchmarked against the code used in Papers I–III with the result that for identical input one gets abundances that agree to within 0.02 dex. In Table 1 we list the adopted atmospheric parameters of our program stars for individual phases, as well as our individual iron abundance (the latter is the same as given in Appendix). In the Appendix (Table A.1) abundances for the stars of the present sample derived from lines of different ions are given along with statistical information about the abundances. Averaged abundances are given in Tables 2–3. Note that the solar abundances are adopted following to Grevesse et al. (1996). Galactocentric distances for program stars were calculated in the same way as in Paper I. They are listed in Table 5.

For the majority of elements studied in the present paper, and especially those whose abundances are based on the analysis of a large number of lines, the standard deviation is less than 0.20 dex. For those with the largest number of lines (such as Si, Fe, and Ni) the standard deviation is generally at the 0.10 dex level (see Appendix). Abundances that were derived from only one or two or at most a few spectral lines, as for example O, Zn, La, Eu, etc., are characterized by larger standard deviations, and the radial distributions of such elements look much less constrained (see Sect. 5).

4. Comparison with previous results

We have previously determined spectroscopic abundances for 5 of the Cepheids considered in this paper: T Mon and RS Ori (Paper I), and XX Mon, TZ Mon, and HW Pup (Paper III). We restrict our attention to Fe (see Appendix) as it is the best determined abundance for these stars. For T Mon, the derived iron abundances (mean) are +0.13 (Paper I) and +0.16 (this work). The T Mon abundances derived here are rather consistent from night to night (+0.11 and +0.21).

Other determinations of the iron content of T Mon give +0.23 (Luck et al. 1998) and -0.03 to $+0.23$ (Luck & Lambert 1985). Given these results one infers that the $[\text{Fe}/\text{H}]$ ratio of T Mon is $\approx +0.15$. For RS Ori the $[\text{Fe}/\text{H}]$ values are -0.10 and -0.02 respectively for our two studies. For XX Mon the respective results are -0.18 and -0.08 , for TZ Mon -0.03 and -0.12 , for HW Pup -0.29 and -0.15 , and for SW Vel $+0.01$ and -0.06 . These values all overlap in terms of their $2\text{-}\sigma$, and there is no evidence from our results for any significant systematic offset between the abundance zero points for data obtained with different spectrographs in our study.

It should be noted that Pont (1997) derived spectroscopic metallicities (specifically $[\text{Fe}/\text{H}]$) for the outer disc Cepheids of Pont et al. (1997). The resulting $[\text{Fe}/\text{H}]$ ratios for 12 objects are given in Table 4. Because these results have been published

Table 1. Program stars: details on the observations and atmospheric parameters.

Star	Date	UT	Exp. (s)	P , d	JD 2452280+	ϕ	T_{eff} , K	$\log g$	V_t , km s $^{-1}$	[Fe I/H]
FI Mon	11	03:35:08	2200	3.2878	5.6494	0.356	5938	2.00	3.5	-0.18
BC Pup	11	06:40:56	2700	3.5443	5.7784	0.062	6695	2.00	3.5	-0.20
BC Pup	12	06:20:38	2700		6.7643	0.341	5879	1.90	3.3	-0.24
FG Mon	11	02:29:31	2700	4.4966	5.6038	0.523	5626	1.60	3.0	-0.20
T Vel	11	08:13:29	80	4.6398	5.8427	0.227	5845	1.90	3.7	-0.04
T Vel	12	08:05:04	160		6.8369	0.441	5570	1.75	3.6	-0.01
WW Mon	12	02:51:09	2400	4.6623	6.6189	0.750	6166	2.20	5.1	-0.29
CU Mon	12	01:46:57	2700	4.7079	6.5743	0.655	5677	1.90	4.5	-0.25
XX Mon	11	06:10:47	1200	5.4565	5.7575	0.211	6060	1.90	3.6	-0.08
TW Mon	11	01:49:26	1800	7.0969	5.5760	0.167	5770	1.70	4.0	-0.24
V510 Mon	11	05:31:36	1800	7.3072	5.7303	0.232	5842	1.40	3.8	-0.19
TZ Mon	11	01:13:18	580	7.4282	5.5509	0.455	5487	1.50	4.0	-0.12
RS Ori	11	04:27:19	80	7.5668	5.6856	0.831	5934	1.85	5.1	-0.02
SX Vel	11	07:57:03	80	9.5499	5.8313	0.354	5578	1.50	3.5	-0.02
SX Vel	12	07:55:31	140		6.8302	0.459	5479	1.60	3.6	-0.04
HW Pup	11	04:38:57	2500	13.4532	5.6937	0.432	5869	1.55	3.6	-0.15
RZ Vel	11	07:50:15	30	20.3969	5.8266	0.988	6549	1.65	6.8	-0.11
RZ Vel	12	07:48:15	60		6.8252	0.037	6669	1.55	6.5	-0.03
SW Vel	11	08:21:26	80	23.4744	5.8482	0.624	5302	1.30	6.1	-0.05
SW Vel	12	07:38:55	150		6.8187	0.666	5224	1.10	5.6	-0.07
T Mon	11	00:48:13	25	27.0205	5.5335	0.562	4853	0.80	4.2	+0.21
T Mon	12	01:29:47	30		6.5623	0.600	4828	1.10	4.7	+0.11
RY Vel	11	07:41:57	60	28.1251	5.8208	0.857	6354	1.50	6.3	-0.03
RY Vel	12	07:30:50	100		6.8131	0.893	6534	1.70	6.4	-0.04
AQ Pup	11	01:05:14	230	29.8568	5.5453	0.756	4937	0.60	5.5	-0.14
AQ Pup	12	07:12:43	240		6.8005	0.798	4958	0.60	5.7	-0.14
RS Pup	11	00:57:21	25	41.3876	5.5398	0.905	5068	1.00	5.0	+0.20
RS Pup	12	06:08:07	50		6.7556	0.935	5073	1.00	4.7	+0.16

Date: January 2002.

Table 2. Averaged relative-to-solar elemental abundance for program Cepheids: C–Mn.

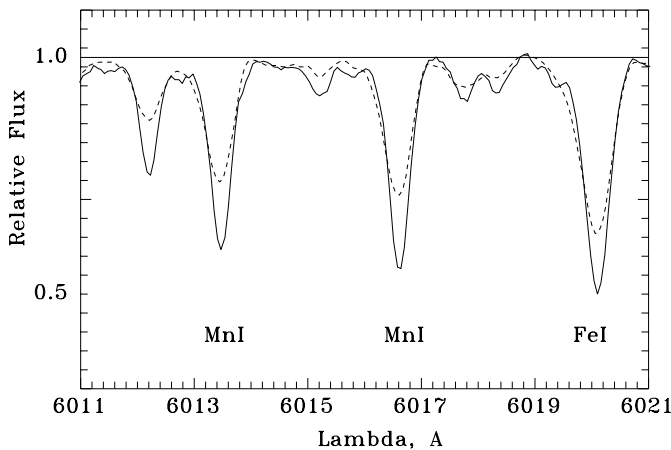
Star	C	N	O	Na	Mg	Al	Si	S	Ca	Sc	Ti	V	Cr	Mn
FI Mon	-0.56	-	-0.41	0.08	-0.03	-0.03	-0.07	-0.14	-0.04	-0.11	-0.06	-0.12	-0.13	-0.24
BC Pup	-0.65	-0.04	-0.55	0.01	-0.30	-0.05	-0.15	-0.27	-0.15	-0.15	-0.10	-0.14	-0.19	-0.19
FG Mon	-0.48	0.26	-0.46	0.09	-0.30	-0.01	-0.10	-0.13	-0.03	-0.23	-0.19	-0.22	-0.11	-0.39
T Vel	-0.28	0.20	0.02	0.06	-0.24	0.08	0.03	0.00	-0.02	-0.09	0.01	-0.14	0.01	-0.14
WW Mon	-0.84	-0.38	-	-0.04	-0.29	-0.27	-0.26	-0.39	-0.26	-0.36	-0.10	-0.40	-	-0.46
CU Mon	-0.52	0.29	-0.06	0.23	-0.36	-0.05	-0.18	-0.36	-0.24	0.02	-0.06	-0.26	-0.06	-0.31
XX Mon	-0.49	0.23	-0.09	0.03	-0.20	0.15	-0.04	-0.15	-0.08	-0.08	-0.16	-0.14	-0.13	-0.19
TW Mon	-0.50	0.00	-0.35	0.01	-0.41	-0.10	-0.17	-0.15	-0.16	-0.29	-0.21	-0.27	-0.16	-0.40
V510 Mon	-0.54	0.01	-0.14	-0.04	-0.27	0.11	-0.10	-0.29	-0.04	-0.34	-0.07	-0.21	-0.24	-0.33
TZ Mon	-0.36	0.37	0.03	0.05	-0.26	0.04	-0.05	-0.07	-0.13	-0.09	-0.08	-0.22	-0.10	-0.23
RS Ori	-0.46	0.29	-0.20	0.06	-0.26	0.07	0.03	-0.02	-0.08	-0.12	-0.10	-0.10	-0.06	-0.11
SX Vel	-0.24	0.17	0.12	0.05	-0.20	0.04	-0.00	0.06	-0.07	-0.00	-0.06	-0.11	-0.04	-0.12
HW Pup	-0.47	0.12	-0.19	0.00	-0.46	-0.04	-0.13	-0.19	-0.22	-0.20	-0.11	-0.12	-0.25	-0.35
RZ Vel	-0.34	0.42	-0.15	0.15	-0.29	0.04	0.07	-0.05	-0.07	-0.27	0.07	-0.04	-0.06	-0.13
SW Vel	-0.45	0.40	-0.01	0.14	0.16	0.13	-0.05	0.04	0.01	0.08	-0.07	-0.09	-0.11	-0.20
T Mon	-0.27	-	0.08	0.35	-	0.19	0.13	0.39	0.03	0.10	0.05	0.02	0.19	0.13
RY Vel	-0.23	0.50	-0.31	0.20	-0.26	0.12	0.06	0.04	-0.11	0.01	-0.02	-0.01	-0.06	0.05
AQ Pup	-0.51	-0.07	-	0.09	-	0.01	-0.10	-0.20	-0.07	-0.05	-0.26	-0.21	-0.17	-0.43
RS Pup	0.03	0.73	0.10	0.42	-	0.17	0.11	0.31	0.21	0.18	0.03	0.00	-0.02	0.13

Table 3. Same as Table 2 but for Fe–Gd.

Star	Fe	Co	Ni	Cu	Zn	Y	Zr	La	Ce	Nd	Eu	Gd
FI Mon	-0.18	0.09	-0.14	-0.18	0.10	0.04	–	0.03	-0.05	0.02	0.11	–
BC Pup	-0.23	-0.03	-0.19	-0.14	-0.20	-0.14	-0.50	0.08	-0.11	0.19	0.21	–
FG Mon	-0.20	-0.16	-0.13	-0.16	0.16	-0.03	-0.34	-0.13	0.03	-0.01	0.01	0.31
T Vel	-0.02	-0.17	-0.08	-0.03	0.29	0.23	-0.22	0.12	0.01	0.02	-0.01	0.03
WW Mon	-0.29	0.03	-0.30	-0.14	-0.04	-0.06	–	0.04	-0.11	0.38	-0.05	–
CU Mon	-0.26	-0.33	-0.27	-0.15	0.10	0.08	–	0.24	0.22	0.13	0.31	–
XX Mon	-0.10	-0.17	-0.10	-0.03	0.23	0.06	-0.15	0.12	0.00	0.09	0.06	0.04
TW Mon	-0.24	-0.18	-0.33	-0.34	0.06	-0.08	-0.29	0.17	-0.18	-0.09	-0.03	–
V510 Mon	-0.19	–	-0.22	-0.08	0.07	-0.09	-0.29	0.00	-0.16	0.02	-0.18	-0.17
TZ Mon	-0.12	-0.18	-0.19	-0.18	0.14	0.08	-0.11	0.16	-0.09	-0.10	0.02	–
RS Ori	-0.08	-0.03	-0.10	0.07	0.21	0.11	-0.12	0.20	-0.13	0.11	0.00	0.07
SX Vel	-0.03	-0.24	-0.09	-0.13	0.27	0.19	-0.15	0.20	-0.07	-0.03	0.00	0.01
HW Pup	-0.20	-0.12	-0.14	-0.19	0.17	-0.01	0.00	-0.08	0.02	0.00	0.07	–
RZ Vel	-0.07	–	-0.06	0.57	0.39	0.08	-0.38	0.31	-0.14	0.08	0.10	–
SW Vel	-0.07	-0.20	-0.11	-0.33	0.30	0.19	-0.08	0.23	-0.14	0.14	0.08	0.12
T Mon	0.13	-0.02	0.08	–	0.34	0.43	0.08	0.29	0.06	0.25	0.19	0.24
RY Vel	-0.03	0.09	-0.01	0.26	0.35	0.17	-0.09	0.29	0.03	0.22	0.19	0.34
AQ Pup	-0.14	-0.34	-0.20	-0.46	–	0.05	-0.33	0.13	-0.17	0.00	0.03	0.12
RS Pup	0.17	-0.01	0.06	-0.09	–	0.18	0.09	0.33	0.09	0.13	0.24	0.13

Table 4. [Fe/H] abundances for distant Cepheids derived by Pont (1997). The common stars are marked by asterisk.

Cepheid	[Fe/H]	R_G	rem.	Cepheid	[Fe/H]	R_G	rem.
AO CMa	-0.02	11.5		WW Mon	-0.25	12.9	*
AA Mon	-0.15	11.2		V447 Mon	-0.22	12.2	
CU Mon	-0.28	14.2	*	V495 Mon	-0.16	12.0	
FT Mon	-0.22	12.4		V510 Mon	-0.20	12.7	*
TW Mon	-0.20	13.5	*	CK Pup	-0.36	13.1	
TZ Mon	-0.24	11.5	*	VW Pup	-0.18	10.3	

**Fig. 1.** Spectra comparison for two Cepheids: *dashed line* – AQ Pup, $\phi = 0.798$, and *solid line* – RS Pup, $\phi = 0.905$ with similar atmosphere parameters, but different metallicities ([Fe/H] = -0.14 and +0.20 respectively).

only in a narrowly circulated document (a Ph.D. Thesis) it is worthwhile to briefly discuss the method.

The cross-correlation function (CCF) was calculated for a series of echelle spectra obtained for outer disc Cepheids with the ELODIE spectrometer at Haute-Provence Observatory, as described in Pont et al. (1997). The equivalent width of the CCF was then used as metallicity indicator. The relation between the CCF equivalent width and [Fe/H] was calibrated with data for solar-neighbourhood Cepheids, with synthetic Cepheid models by M. Albrow (priv. comm.) and with spectra of SMC Cepheids (assuming [Fe/H]_{SMC} = -0.6 dex) obtained with the ESO New Technology Telescope. The $(V-I)_0$ colour was used as a temperature indicator. Several schemes were considered for the determination of reddening (outer disc cepheids are heavily reddened), and the most reliable method was found to be via a comparison of the distance modulus from the K magnitude with the observed colours, the absorption in the K band being very small. The K magnitudes were obtained with the 1.9 m telescope at the SAAO in Sutherland, South Africa.

The CCF values of [Fe/H] are in excellent agreement with the high- S/N spectroscopic values of the present paper. For the five objects in common, the dispersion is 0.04 dex, giving further confidence in the accuracy of both determinations.

Table 5. Physical and positional characteristics for program Cepheids.

Star	P , d	d , pc	l	b	M_V	R_G , kpc	[Fe/H]
FI Mon	3.2878	6034	221.48	1.02	-2.73	13.05	-0.18
BC Pup	3.5443	5990	238.26	-2.67	-2.82	12.16	-0.23
FG Mon	4.4966	6895	221.65	-0.09	-3.10	13.83	-0.20
T Vel	4.6398	1121	265.55	-3.78	-3.14	8.06	-0.02
WW Mon	4.6623	5241	202.71	0.27	-3.15	12.89	-0.29
CU Mon	4.7079	6866	210.76	-4.13	-3.16	14.22	-0.26
XX Mon	5.4565	4567	215.52	-1.11	-3.33	11.92	-0.10
TW Mon	7.0969	6150	212.82	-0.19	-3.65	13.49	-0.24
V510 Mon	7.3072	5229	210.24	0.26	-3.69	12.69	-0.19
TZ Mon	7.4282	4021	214.01	1.29	-3.71	11.45	-0.12
RS Ori	7.5668	1499	196.58	0.35	-3.73	9.35	-0.08
SX Vel	9.5499	1944	265.49	-2.18	-4.01	8.28	-0.03
HW Pup	13.4532	6684	244.77	0.78	-4.42	12.33	-0.20
RZ Vel	20.3969	1508	262.88	-1.91	-4.92	8.22	-0.07
SW Vel	23.4744	2572	266.20	-3.00	-5.09	8.47	-0.07
T Mon	27.0205	1370	203.63	-2.55	-5.26	9.17	+0.13
RY Vel	28.1251	2335	282.57	1.48	-5.31	7.74	-0.03
AQ Pup	29.8568	3114	246.16	0.11	-5.39	9.59	-0.14
RS Pup	41.3876	1756	252.43	-0.19	-5.77	8.59	+0.17

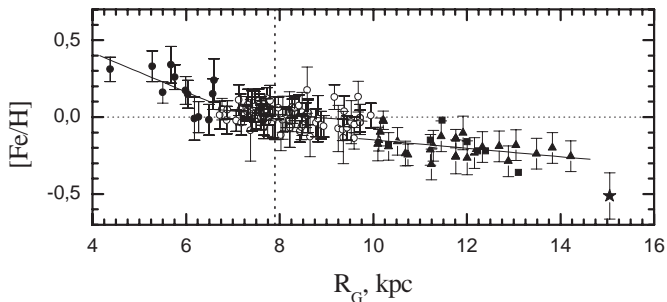


Fig. 2. The radial distribution of the iron abundance. *Open circles* – the data from Paper I (the positions of some stars were corrected (vertical shift) taking into account the results of the present study), *black circles* – the data from Paper II, *black triangles* – present results combined with data from Paper III. $2\text{-}\sigma$ interval is indicated (the standard error of the mean, i.e. $\frac{\sigma}{\sqrt{N}}$, is of the order of 0.01). The position of EE Mon is indicated by *filled asterisk*. The Sun is marked by the intersection of the dashed lines. The data from Pont (1997) are indicated by filled squares (only the stars that were not investigated in present paper).

5. Abundance distributions

To find the element distribution in the galactic disc we used the elemental abundances (Tables 2, 3) and galactocentric distances from Table 5 (this table has data only for the stars whose abundances were derived in this paper – for the remaining stars see Papers I-III). Note, that in the case of common stars between Papers I, III and the present study, we

calculated the mean abundances from all available determinations. The average abundances are given in Tables 2, 3, and they may slightly differ from the values (derived from this analysis only) given in the Appendix.

The radial distributions obtained in this way are presented by Figs. 2–6. Following Paper III we adopted special symbols to distinguish the stars from the different domains of the galactic disc. Several stars from the new sample are at galactocentric distances placing them near the solar galactic orbit (see Table 5). These stars have a metallicity which is similar to that of the Cepheids with $R_G \approx 8$ kpc. One star in this region (RS Pup), however, appears to be enriched in metals. Its position resembles that of another metal-rich Cepheid, T Mon, reported in Paper I. These two stars may serve as preliminary indicators of the existence of rather significant local chemical inhomogeneities in the ISM. It should, however, be noted that RS Pup and T Mon are both long-period Cepheids, and therefore may be younger than the other, shorter-period Cepheids; this could imply that their younger age could contribute somewhat to their observed increased metal abundances.

Another case is CF Cas with its position at about 9.7 kpc (similar to T Mon and RS Pup; Fig. 14 in Paper I and Fig. 2 in the present paper). However, the abundances for this star bear less weight because they are based on a lower resolution spectrum and could be somewhat overestimated (note that this star in the overall statistics is assigned a weight $W = 1$, the remaining stars discussed here have a weight $W = 3$ – see Paper I for a discussion of assigned weights). Therefore the abundances for this Cepheid must be regarded with some caution.

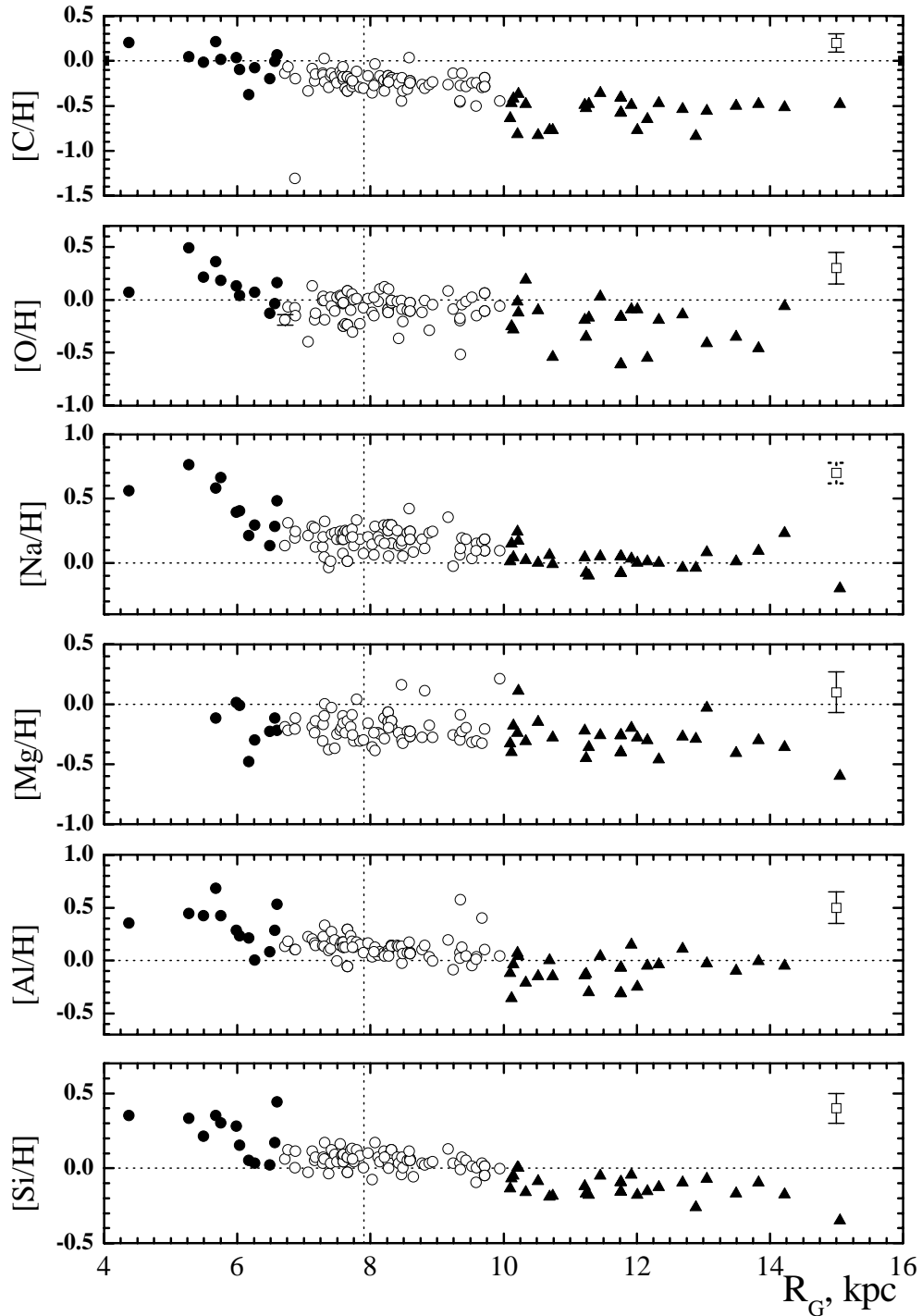


Fig. 3. Same as Fig. 2, but for elements C–Si. The typical individual 2σ interval is indicated.

The abundance deviations, which are seen at some galactocentric distances, may reflect real small-scale abundance inhomogeneities in the interstellar medium. It would be very interesting to use the Cepheid data in an investigation of the longitudinal metallicity distribution at given galactocentric distances (similar to Paper I, but with higher resolution on R_G). Nevertheless, we think that the present sample of observed Cepheids is insufficient to approach this problem.

Even though some elemental abundances are expected to be modified due to evolution in the supergiants, they still show clear gradients. Among such elements are carbon and magnesium whose nuclei are exhausted in the CNO- and MgAl- cycles (most of the Cepheids are carbon-magnesium deficient stars), and nitrogen and sodium (both are enhanced in Cepheids as a result of CNO- and NeNa – cycle operation). Since the real level of depletion/enhancement of these elements

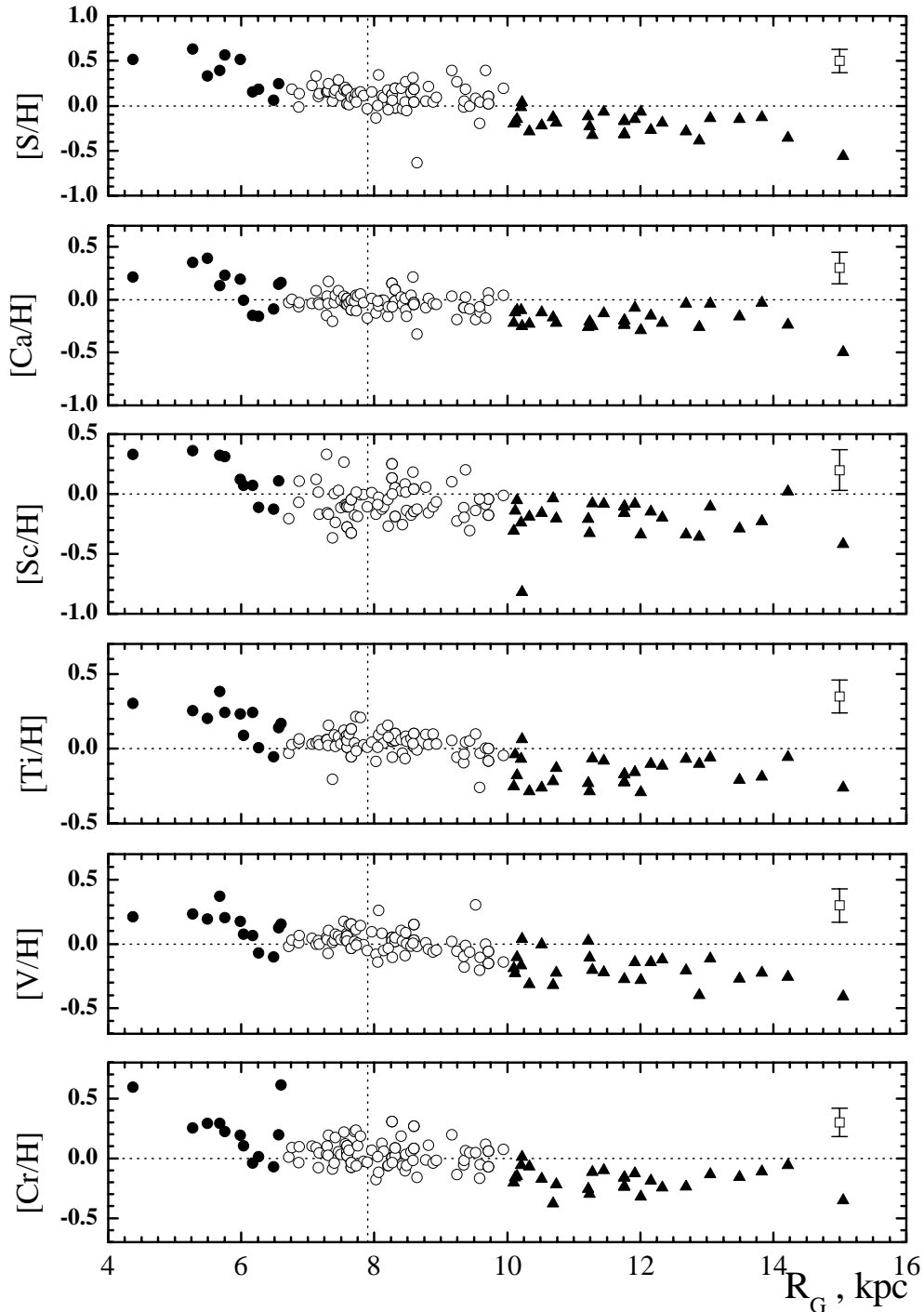


Fig. 4. Same as Fig. 2, but for elements S–Cr.

(compared to the ISM) in a given Cepheid is not known, their gradients should be taken and interpreted with caution.

Our improved data on the metallicity distribution (especially iron one) in the galactic disc over the galactocentric distance range 10 kpc–14 kpc support the existence of a discontinuity at $R_G \approx 10$ kpc, which was first claimed by Twarog et al. (1997), then noted by Caputo et al. (2001), and further confirmed in Paper III, in the sense that the metallicity

drops quite suddenly from about solar to ≈ -0.2 dex near this value of galactocentric distance.

The discontinuity is also clearly seen in Fig. 7 where the iron distribution is presented along a piece-wise smoothed (15-points) line. The smoothing was performed using the LOWESS method. A local regression model is fit to each point and the points close to it.

To evaluate the significance level of the discontinuity existence one can compare the mean abundances for the middle

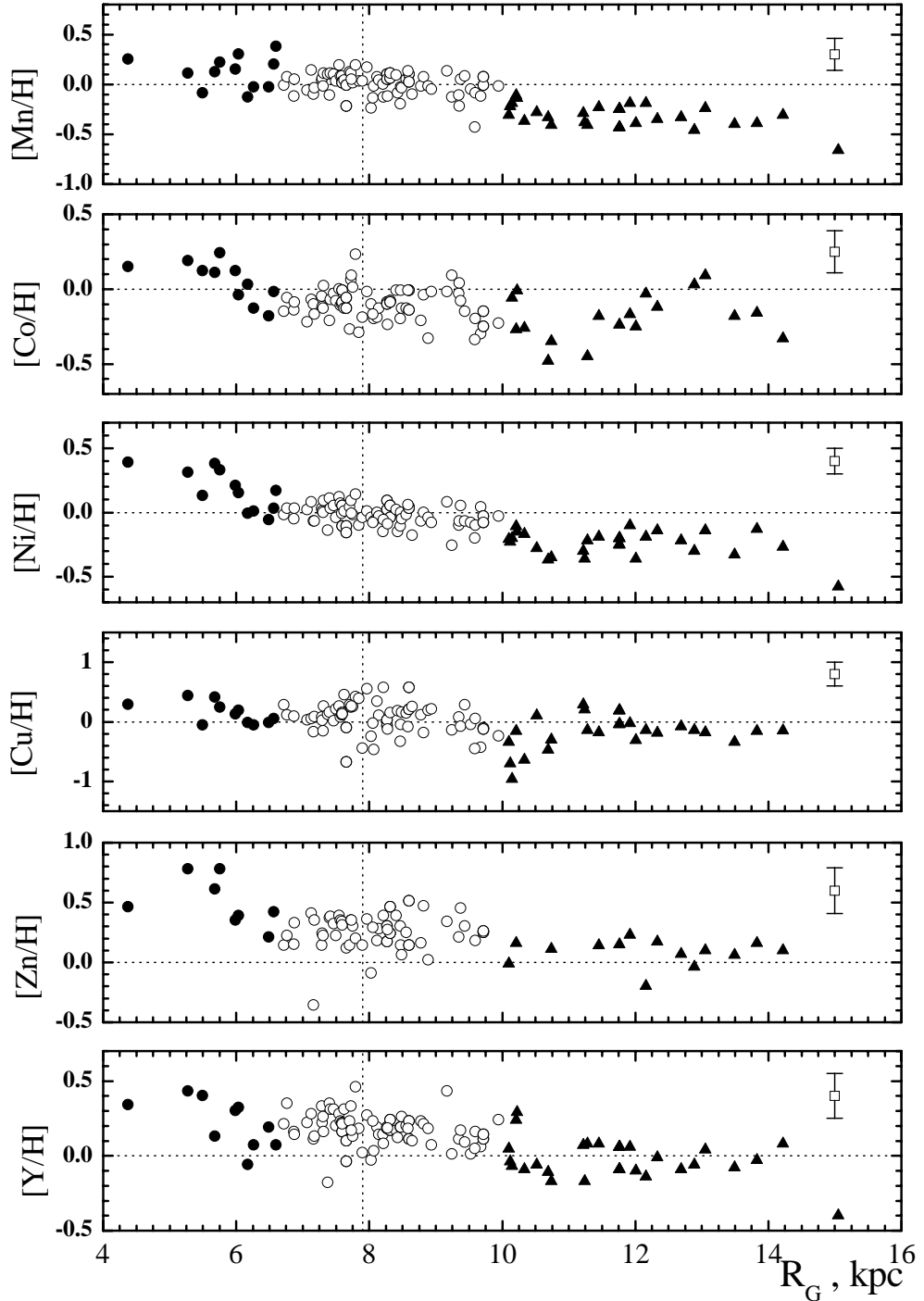


Fig. 5. Same as Fig. 2, but for elements Mn–Y.

and outer parts of the disc using the t-criterion (although such a comparison perhaps cannot be completely correct, since some contribution to the difference of two mean abundances may artificially come from the non-zero slopes of the distributions in the middle and outer zones, even though the slopes are quite small). For this one can calculate for each elemental distribution (Figs. 2–6) the following value:

$$t = \frac{[\text{E}/\text{H}]_{\text{mid}}^{\text{mean}} - [\text{E}/\text{H}]_{\text{out}}^{\text{mean}}}{\sqrt{\frac{s^2}{n_{\text{mid}}} + \frac{s^2}{n_{\text{out}}}}}.$$

Here s is the combined standard deviation:

$$s^2 = \frac{\sum_{i=1}^{n_{\text{mid}}} \left([\text{E}/\text{H}]_{\text{mid}}^i - [\text{E}/\text{H}]_{\text{mid}}^{\text{mean}} \right)^2}{n_{\text{mid}} + n_{\text{out}} - 2} + \frac{\sum_{i=1}^{n_{\text{out}}} \left([\text{E}/\text{H}]_{\text{out}}^i - [\text{E}/\text{H}]_{\text{out}}^{\text{mean}} \right)^2}{n_{\text{mid}} + n_{\text{out}} - 2} \quad (2)$$

(1) and n_{mid} and n_{out} – are the number of stars in two zones. In Table 6 we present the results of such an evaluation. In the

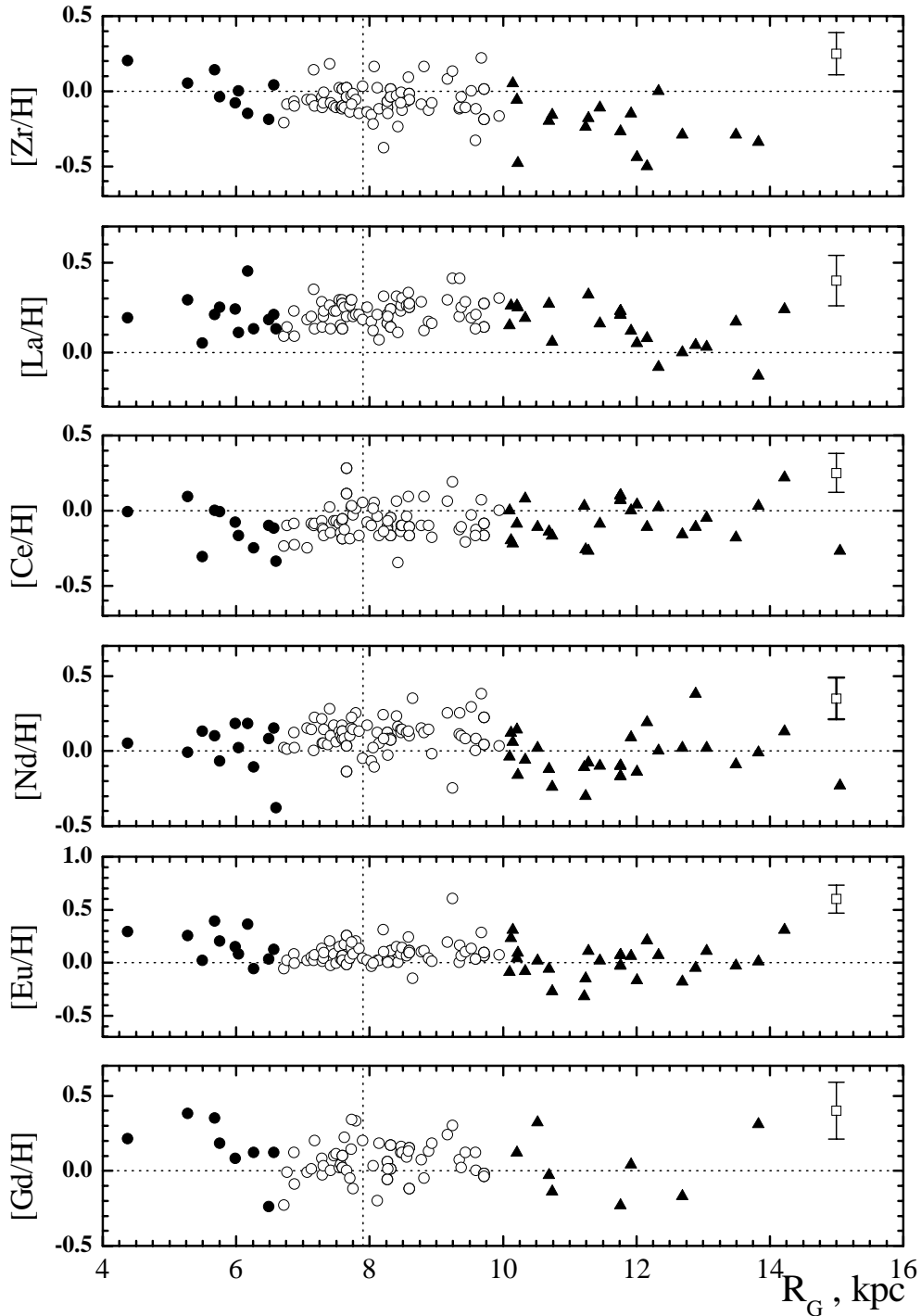


Fig. 6. Same as Fig. 2, but for elements Zr–Gd.

final column of Table 6 we give a conclusion as to whether or not the two mean values are significantly different. This conclusion is based on a comparison of calculated t -values with tabulated one $t^T = 2.57$ (with a probability of 0.01 and degrees of freedom $\nu \rightarrow \infty$). Two mean values differ significantly if $t > t^T$. From the statistics for carbon we excluded the abundance result for FN Aql. The same was made for sulphur (VX Pup) and scandium (GQ Ori). These stars have an apparent anomaly in abundances of these elements. The results give

some reason to believe that the discontinuity is real. However, the result for iron (for example) depends strongly on the iron abundances at about $R_G = 11$ kpc. More stars in this vicinity in particular are needed to make the discontinuity result more robust.

A discontinuity could be a consequence of the specific initial conditions of the Galaxy formation (thick and thin disc separation), and might have survived over the long-term period if

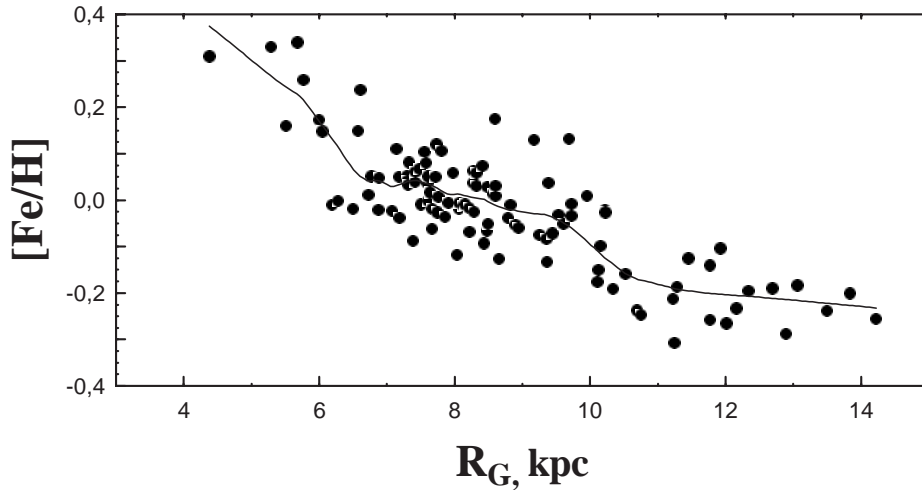


Fig. 7. Smoothed data for iron abundance distribution.

Table 6. Statistical characteristics of the radial distributions. Mean abundances and individual σ -values for each zone are given.

Element	mid		out		t	rem.
	mean	σ^2	mean	σ^2		
C	-0.248	0.028	-0.574	0.021	14.8	yes
O	-0.077	0.015	-0.226	0.041	7.1	yes:
Na	+0.180	0.008	+0.030	0.008	12.5	yes
Mg	-0.188	0.014	-0.289	0.013	6.0	yes:
Al	+0.119	0.007	-0.091	0.017	15.3	yes
Si	+0.053	0.003	-0.128	0.004	22.8	yes
S	+0.105	0.015	-0.200	0.011	19.1	yes
Ca	-0.022	0.006	-0.176	0.007	14.0	yes
Sc	-0.062	0.020	-0.195	0.017	6.9	yes:
Ti	+0.034	0.005	-0.159	0.007	18.3	yes
V	+0.007	0.007	-0.197	0.011	16.3	yes
Cr	+0.040	0.010	-0.181	0.008	16.3	yes
Mn	+0.009	0.012	-0.313	0.010	22.1	yes
Fe	+0.010	0.004	-0.192	0.005	22.9	yes
Co	-0.107	0.011	-0.200	0.024	4.9	yes:
Ni	-0.017	0.006	-0.238	0.008	20.2	yes
Cu	+0.077	0.061	-0.203	0.080	7.8	yes:
Zn	+0.259	0.020	+0.086	0.011	7.3	yes:
Y	+0.189	0.009	-0.024	0.013	15.4	yes
Zr	-0.071	0.010	-0.218	0.023	7.9	yes:
La	+0.218	0.005	+0.133	0.014	6.7	yes:
Ce	-0.085	0.011	-0.068	0.016	1.1	not
Nd	+0.106	0.008	-0.021	0.021	8.6	yes:
Eu	+0.075	0.007	+0.007	0.026	4.5	yes:
Gd	+0.061	0.013	+0.028	0.041	1.2	not

the mixing process smoothing the metallicity differences was not efficient in this particular region near $R_G \approx 10$ kpc.

In the vicinity of this region the mixing processes can be efficiently suppressed by the density gap associated with the corotation resonance (see Paper III). Near the corotation circle the radial component of the gas velocity should be very small (no mixing in radial direction), and this circumstance should in addition favour the preservation of a boundary between the thick and thin disc.

Taking the range from 10 kpc to 14 kpc as the boundaries of a separate domain of the galactic disc, and combining the data from the present paper with those of Paper III, one can derive the iron abundance gradient in this region as -0.03 ± 0.01 dex kpc^{-1} with the mean abundance $\langle[\text{Fe}/\text{H}]\rangle = -0.18 \pm 0.07$ (the very distant Cepheid EE Mon is excluded).

Summarizing the results from our work on Cepheid abundances (iron, in particular, as the most reliable abundance) in the galactic disc, the emerging picture is that there is a relatively steep gradient (about -0.14 dex kpc^{-1}) for R_G less than 7 kpc, a much shallower gradient (≈ -0.03 dex kpc^{-1}) between 7 and 10 kpc, and a discontinuity at approximately 10 kpc which is followed by a near-constant metallicity of about -0.2 dex towards larger galactocentric distances, out to about 14 kpc. The sole Cepheid in our sample clearly beyond 14 kpc, EE Mon, provides some evidence that the metallicity in the galactic disc might drop further at very large galactocentric distances, but this has to be confirmed by further studies of extremely distant objects in the outer galactic disc.

Acknowledgements. We are grateful to the European Southern Observatory for the allocation of observing time to this project. We would also like to thank the NTT team, and in particular Olivier Hainaut, for excellent support at the telescope. W.G. gratefully acknowledges financial support for this work from the Chilean Center for Astrophysics FONDAF 15010003. SMA is thankful to FAPESP for supporting grant 1998/10138-8. REL and SMA acknowledge financial support from a Chretien International Research Grant (administered by the American Astronomical Society).

The authors thank the anonymous referee for valuable comments.

References

- Andrievsky, S. M., Kovtyukh, V. V., Luck, R. E., et al. 2002a, *A&A*, 381, 32 (Paper I)
- Andrievsky, S. M., Bersier, D., Kovtyukh, V. V., et al. 2002b, *A&A*, 384, 140 (Paper II)
- Andrievsky, S. M., Kovtyukh, V. V., Luck, R. E., et al. 2002c, *A&A*, 392, 491 (Paper III)
- Caputo, F., Marconi, M., Musella, I., & Pont, F. 2001, *A&A*, 372, 544
- Chiappini, C., Matteucci, F., & Romano, D. 2001, *ApJ*, 554, 1044
- Gieren, W. P., Fouqué, P., & Gómez, M. 1997, *ApJ*, 488, 74
- Gieren, W. P., Fouqué, P., & Gómez, M. 1998, *ApJ*, 496, 17
- Grevesse, N., Noels, A., & Sauval, J. 1996, *ASP Conf. Ser.*, 99, 117
- Lang, K. R. 1974, *Astrophysical formulae* (Springer-Verlag)
- Luck, R. E., & Lambert, D. L. 1985, *ApJ*, 298, 782
- Luck, R. E., Moffet, T. J., Barnes, III T. G., & Gieren, W. P. 1998, *ApJ*, 115, 605
- Pont, F. 1997, Ph.D. Thesis, Genève
- Pont, F., Queloz, D., Bratschi, P., & Mayor, M. 1997, *A&A*, 318, 416
- Pont, F., Kienzle, F., Gieren, W., & Fouqué, P. 2001, *A&A*, 376, 892
- Snedden, C. 1973, Ph.D. Thesis, Univ. Texas Austin
- Twarog, B. A., Ashman, K. M., & Antony-Twarog, B. J. 1997, *AJ*, 114, 2556
- Van den Bergh, S. 1958, *AJ*, 63, 492